Transient Critical Heat Fluxes in Subcooled Pool Boiling of FC-72

Sutopo, Purwono F.
Fukuda, Katsuya
Liu, Qiusheng

Journal of Power and Energy Systems

Vol. 2, No. 2, 2008

Transient Critical Heat Fluxes in Subcooled Pool Boiling of FC-72*

Purwono Fitri SUTOPO**, Katsuya FUKUDA*** and Qiusheng LIU***

**Graduate School of Science and Technology, Kobe University
5-1-1, Fukaeminami, Higashinada, Kobe, Hyogo 658-0022 Japan
***Graduate School of Maritime Sciences, Kobe University
5-1-1, Fukaeminami, Higashinada, Kobe, Hyogo 658-0022 Japan
E-mail: fukuda@maritime.kobe-u.ac.jp

Abstract

Critical heat fluxes (CHFs) in a pool of Fluorinert FC-72 were measured for period from transient heat inputs up to steady-state ones. Measurements were made using 1.0 mm diameter of platinum and gold horizontal cylinders in wide ranges of liquid subcoolings and pressures. The steady-state CHFs for saturated condition almost agree with the hydrodynamic instability (HI) model. However, in higher subcoolings, the increasing rate of steady-state CHFs is lower than HI model and it was suggested due to the heterogeneous spontaneous nucleation (HSN). The CHFs for period are clearly categorized into the first, second, and third groups for long, short, and intermediate periods, respectively. Transient CHFs on semi-direct and direct transitions from non-boiling heat conduction to film boiling, exist predominantly during short periods. Those transition processes were assumed due to the explosive-like HSN in originally flooded cavities on cylinder surface. Each of the steady-state and transient CHFs that were obtained from both heaters in various liquid subcoolings and pressures, generally well agree each other.

Key words: Transient CHF, Subcooling, Pool Boiling, Horizontal Cylinder, FC-72

1. Introduction

Extensive investigations toward critical heat flux (CHF) in boiling heat transfer processes have been widely performed. However, the correct understanding of CHF phenomenon during the steady-state and transient heat transfer, as a fundamental database for designing heat generation systems still needs to be clarified, especially in relation to design and safety evaluation of nuclear reactor.

Studies of CHFs in pool of highly wetting liquids due to transient heat inputs (exponentially increasing of heat rates ranging from quasi-steady to rapidly increasing ones) for a wide range of subcoolings and pressures have been performed. Typical trend of CHF corresponds to periods is as follows: the CHF slightly increases up to maximum CHF from a steady-state CHF (a condition of CHF that corresponds to a period of 10 s or more), then decreases down to a minimum CHF and finally increases again with the decrease in period. Its trend was generally classified into three separate groups are the first group, second, and third groups, for long, short, and intermediate periods, respectively[(1)-(3),(5)-(8)].

The CHFs in a pool of wetting liquid of FC-72 due to transient heat inputs for the wide range of subcoolings and pressures have been also investigated[(2)]. Steady-state and transient CHFs were measured on 1.2 mm diameter platinum horizontal cylinder for pressures ranging from atmospheric to 150 kPa and subcoolings from 0 to 50 K. The transient CHFs for longest period of the second group for each subcooling are about

*Received 3 Sep., 2007 (No. 07-0491)
[DOI: 10.1299/jpes.2.804]

one-tenth of the steady-state ones. The steady-state CHFs within the tested range showed an increase by the increase in subcoolings but less dependence on the pressure.

Recently, the transient CHFs in a pool of saturated and subcooled of wetting liquids of FC-72 and ethanol using 1.0 mm diameter horizontal cylinders were measured to investigate the effect of liquid subcoolings on the steady-state and transient CHFs[(1),(3),(6)-(8)]. The steady-state CHFs were dependent on pressures and almost agree with the values obtained by Kutateladze's correlation based on the hydrodynamic instability (HI) model at around zero subcooling.

The direct transition processes to film boiling without nucleate boiling for the short periods were confirmed due to the HSN process in flooded cavities on the cylinder surface[(1)-(3),(5)-(8)]. It was found also that in the pool of highly wetting liquids, the incipient boiling process during transition to fully developed nucleate boiling for periods of above 10 s at around atmospheric pressure was caused by the flooded cavities on cylinder surface rather than active cavities[(1)-(3),(5),(7),(8)]. At atmospheric pressure, the fluorinert liquid FC-72 is a highly wetting liquid that has 0.008 N/m of surface tension property, lower than liquid nitrogen, ethanol, and about one-eighth lower than water. Its contact angle between liquid and heater surface is smaller than that of water, so that it is expected the inception of boiling may occur due to HSN in flooded cavities on a solid surface in FC-72.

In this study, experiments were performed to investigate the characteristics of the steady-state and transient CHFs due to increasing heat inputs under a wide range of liquid subcoolings and pressures on different horizontal cylinders in the wide range of exponential periods.

2. Nomenclature

a	thermal diffusivity, m^2/s
c_{pl}	specific heat at constant pressure, J/kgK
d	cylinder diameter, m
g	acceleration of gravity, m/s^2
K_1	constant in Eq. (4)
K_2	constant in Eq. (3)
K_3	constant in Eq. (6)
k	thermal conductivity, W/mK
Q	heat generation rate, W/m^3
Q_0	initial exponential heat input, W/m^3
q	heat flux, W/m^2
q_{cr}	CHF, W/m^2
$q_{st,sat}$	steady-state CHF for saturated condition, W/m^2
$q_{st,sub}$	steady-state CHF for subcooled condition, W/m^2
R	characteristic cylinder radius, m
R'	$(R[g(\rho_l-\rho_v)/\sigma]^{1/2})$, dimensionless characteristic radius
r	cylinder radius, m
T	temperature inside the test heater, K
T_m	average temperature of the test heater, K
T_w	heater surface temperature, K
T_{sat}	saturation temperature, K
ΔT_{sat}	(T_w-T_{sat}), surface superheat, K
ΔT_{sub}	$(T_{sat}-T_{Bulk})$, liquid subcooling, K
t	time, s
λ	heater thermal conductivity, W/mK
ρ	density, kg/m^3

σ surface tension, N/m
τ exponential period, s
μ $(\rho_l c_{pl}/k_l\tau)^{0.5}$, m^{-1}

Subscripts
h heater
l liquid
v vapor

3. Experimental Method and Apparatus

3.1 Apparatus and test section

The pool boiling experimental apparatus is shown schematically in Fig. 1. It mainly consists of a boiling vessel and a test section inside the vessel, a pressurizer, the heat generation rate controlling system, the measurement and data processing system, and a high-speed video camera.

Experiments were performed on the test section of platinum and gold cylinders with a diameter of 1.0 mm. The test section is horizontally mounted inside the boiling vessel. Two fine 50 μm diameter wires were spot welded at about 10 mm apart from each terminal of the test heaters as potential taps. The effective lengths between the potential taps are about 30 mm for both heaters. The test heater was annealed and the electrical resistance and temperature relation was calibrated using a precision double bridge circuit in water and glycerin baths. The calibration accuracy was estimated to be within ±0.5 K.

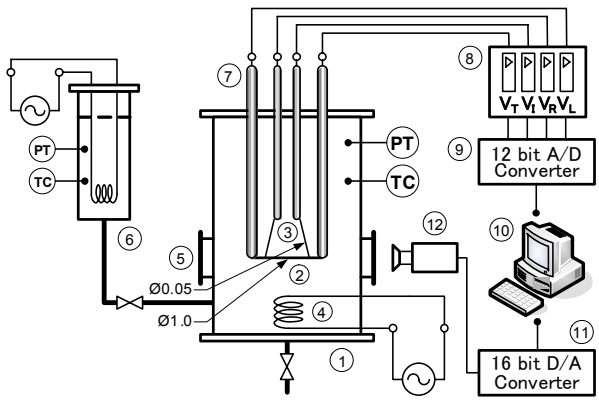

Fig. 1 Schematic diagram of experimental apparatus

3.2 Experimental method and procedure

The test heater was heated electrically by using a fast response, direct current source (max. 700 A) controlled by a digital computer so as to give increasing heat input with a period. The average temperature of the test heaters was measured by resistance thermometry using the heater itself. A double bridge circuit with the heater as a branch was first balanced at the bulk liquid temperature. The output voltages of the bridge circuit, together with the voltage drops across the potential taps of the heater and across a standard resistance, were amplified and passed through analog-to-digital converters of a personal

computer. These voltages were simultaneously sampled at a constant time interval. The average temperature was obtained by using the previously calibrated resistance-temperature relation.

The heat generation rate of the test heater was determined from the current to the heater and the voltage difference between potential taps on the test heaters. The surface temperature was obtained by solving the conduction equation in the heater under the conditions of the average temperature and heat generation rate. The instantaneous surface heat flux was obtained from the heat balance equation for a given heat generation rate. The experimental error was estimated to be about ±1 K in the heater surface temperature and ±2 % in the heat flux.

The experiment was carried out as follows. First, a boiling process for degassing of the liquid used in the experiment was performed at least for 30 minutes. Then, the liquid was fully filled in the boiling vessel with the free surface only in the pressurizer and liquid feed tank. Liquid temperatures and pressures in the boiling vessel and in the pressurizer were separately controlled to realize the desired saturated and subcooled conditions. At pressures more than atmospheric one, those experimental conditions were controlled by raising of liquid temperature, and the pressurization was carried out by the steam itself.

The electric current was supplied to the test heater, and the heat generation rate, Q, increased with exponential function, $Q=Q_0e^{t/\tau}$. The heat input control system then controls and measures the heat generation rate of the heater. The average temperature of test heater was measured by resistance thermometry using a double bridge circuit including the test heater as a branch. The heat flux of the heater was calculated by the following equation for heat balance.

$$q = \frac{d}{4}Q - \rho_h c_h \frac{d}{4}\frac{dT_m}{dt} \tag{1}$$

The test heater surface temperature can be calculated from unsteady heat conduction equation of the next expression by assuming the surface temperature around the test heater to be uniform. For the cylindrical test heater, we have,

$$\frac{\partial T}{\partial t} = a\left(\frac{\partial^2 T}{\partial r^2} + \frac{1}{r}\frac{\partial T}{\partial r}\right) + \frac{Q}{\rho_h c_h} \tag{2}$$

A high-speed video camera system (1000 frames/s with a rotary shutter exposure of 1/10000 s) was used to observe the boiling phenomena and to confirm the start of boiling on the test heater surface. The high-speed video camera was started before the starting of a measurement. A video timer started simultaneously with the starting of measurement, then the boiling phenomenon was recorded with the passage of time.

4. Results and Discussion

4.1 Experimental conditions

Pool boiling experiments were set up on a horizontal test heater in a pool of FC-72 due to transient heat inputs, for the exponential periods, τ, ranging from 10 ms up to 20 s. In the experiments, authors used 1.0 mm diameter horizontal platinum and gold cylinders as the test heaters. The system parameters of experiment cover a wide range of liquid subcoolings from 0 to 140 K, and system pressures ranging from 101.3 kPa to 1278.1 kPa for platinum cylinder, and from 101.3 kPa to 1082.0 kPa for gold cylinder.

4.2 Boiling heat transfer processes

Typical of boiling heat transfer processes including CHFs are shown in Fig. 2 which represents the characteristics of heat flux, q, versus surface superheat, ΔT_{sat}, and were measured on 1.0 mm diameter horizontal cylinders in a pool of FC-72 due to transient heat inputs in various parameters of pressures and liquid subcoolings.

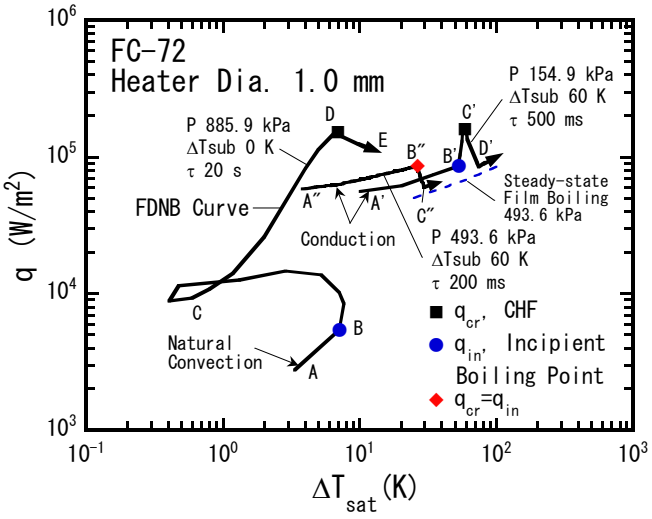

Fig. 2 Boiling heat transfer processes in a pool of FC-72 due to transient heat inputs

The typical heat transfer process with a transition from non-boiling regime to film boiling through fully developed nucleate boiling (FDNB) caused by quasi-steadily increasing natural convection regime, namely type 1, is shown in figure represented by the steady-state boiling curve corresponds to period of 20 s, which was obtained at zero subcooling and pressure of 885.9 kPa. At first, during process A-B, q increases along natural convection curve. After boiling initiation at point B, boiling hysteresis appears through process B-C due to the activation of originally flooded cavities during boiling incipience which induces a rapid growing of vapor film covering the cylinder surface accompanied by a rapid change of surface superheat and heat flux, then followed by large detachment of bubbles before onset of nucleate boiling at C[4]. The heat flux then increases gradually along the steady-state FDNB curve up to the CHF, point D, accompanied by an increase of surface superheat. The transition from FDNB to film boiling occurs due to the hydrodynamic instability (HI) in the two-phase region near the cylinder surface[10],[11].

The type 1 of boiling heat transfer process predominantly occurs at quasi steady-state periods of $\tau > 1000$ ms in saturated and whole subcooled conditions. At high pressures around above 493.6 kPa for low and high subcoolings on both heaters, the CHFs, q_{cr}, from FDNB process belongs to the type 1, seem to appear in shorter periods. Those characteristics can be seen effectively in graph of q_{cr} versus exponential periods, τ, in Figs. 6 and 7. However, a tendency toward an insufficient forming of nucleate boiling may lead to decreasing value of CHF lower than the steady-state ones. Thus, it may appear as CHFs belong to the third group on intermediate period between short and long periods.

The direct transitions from non-boiling regime to film boiling process, namely type 2, due to transient heat input to the heater, predominantly occur within short periods of τ. As seen in Fig. 2, the type 2 of typical boiling processes are represented by the graph of boiling curve due to transient heat input for setting periods of 200 ms at period of 493.6 kPa and liquid subcooling of 60 K. The non-boiling process increases up to CHF at point B" and agrees well with the heat flux values derived by transient heat conduction presented by Sakurai and Shiotsu (1977). Then, the heat flux decreases down to minimum value, and finally again achieves the stable film boiling with rapid increase of surface superheat. The direct

transition process with a simultaneously process of CHF after boiling was assumed due to the explosive-like HSN in originally flooded cavities on the cylinder surface[5].

The direct transitions occur in vary ranges of short periods and it can be seen representatively by graphs of q_{cr} versus exponential periods, τ, in Figs. 6 and 7. As seen in both figures, in high pressures, the longest periods belong to the second groups of CHFs shorten with the increase in pressure.

The type 3 of typical boiling process was observed for a transition from non-boiling regime to film boiling through short nucleate boiling with an increasing heat flux. In Fig. 2, the type 3 of typical boiling processes are represented by the graph of boiling curve for setting period of 500 ms at pressure of 154.9 kPa and liquid subcooling of 60 K. The non-boiling process increases up to point B'. The non-boiling heat flux changes suddenly at the inception of boiling at point B' up to point C', with a small increase of surface superheat. The heat flux then drops down to minimum heat flux that approaching a stable film boiling. The transition to film boiling through nucleate boiling that is not FDNB is called semi-direct transition. This type predominantly appears in short periods region belong to the second group, and it can be seen in Fig. 7. The semi-direct transitions in a pool of subcooled FC-72 are assumed due to slight nucleate boiling from active cavities on surface heater which give increasing of heat flux, then diminish with surface superheat after CHF is reached where the explosive-like heterogeneous nucleation predominate since boiling initiation.

The steady-state film boiling at pressure in the pool boiling heat transfer process was obtained from the theoretical pool film boiling heat transfer model with radiation contribution from the horizontal cylinder[9].

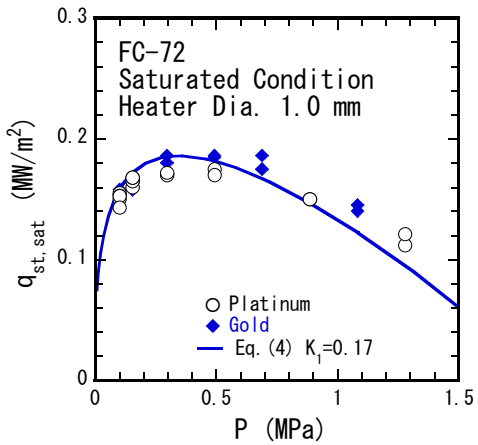

Fig. 3 The Steady-state CHFs vs pressures under saturated FC-72 on 1.0 mm diameter cylinders

4.3 Steady-state critical heat fluxes

The heat transfer processes for the periods longer than 10 s were considered as steady-state ones because the non-boiling regime agrees with natural convection heat transfer processes, and they have an almost constant rate of CHFs that less dependent on periods.

4.3.1 Saturated condition

The steady-state CHFs, $q_{st,sat}$, under saturated conditions at a wide range of pressures, P, from atmospheric pressure up to 1278.1 kPa are shown in Fig. 3. The CHFs almost agree with the corresponding values based on HI model that were calculated from Eq. (4). However, in high pressures above 493.6 kPa, they give a slight higher of increasing rate rather than the corresponding ones. More additional descriptions for saturated condition have been reported elsewhere by authors[7].

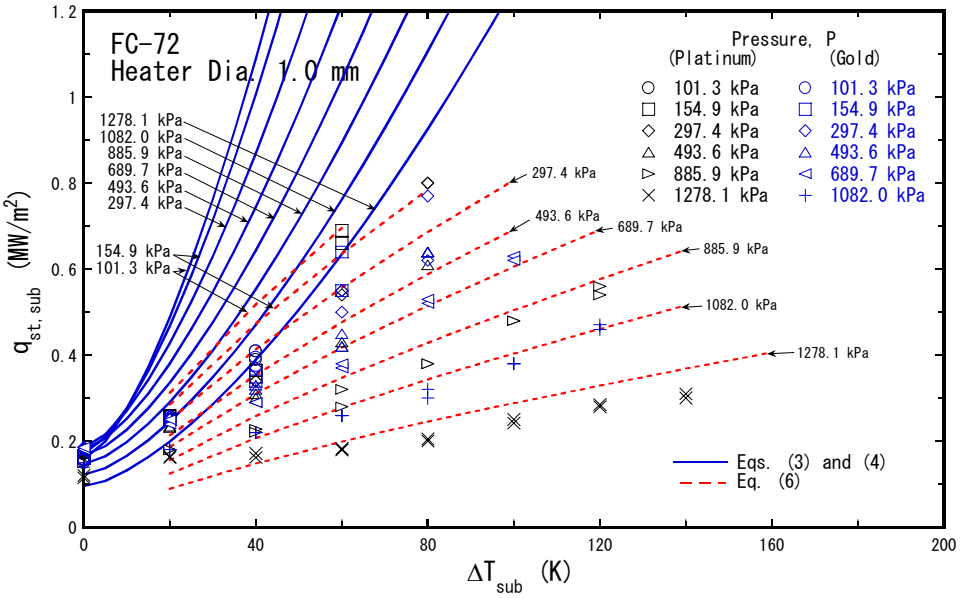

Fig. 4 The Steady-state CHFs for liquid subcoolings with pressure as parameter

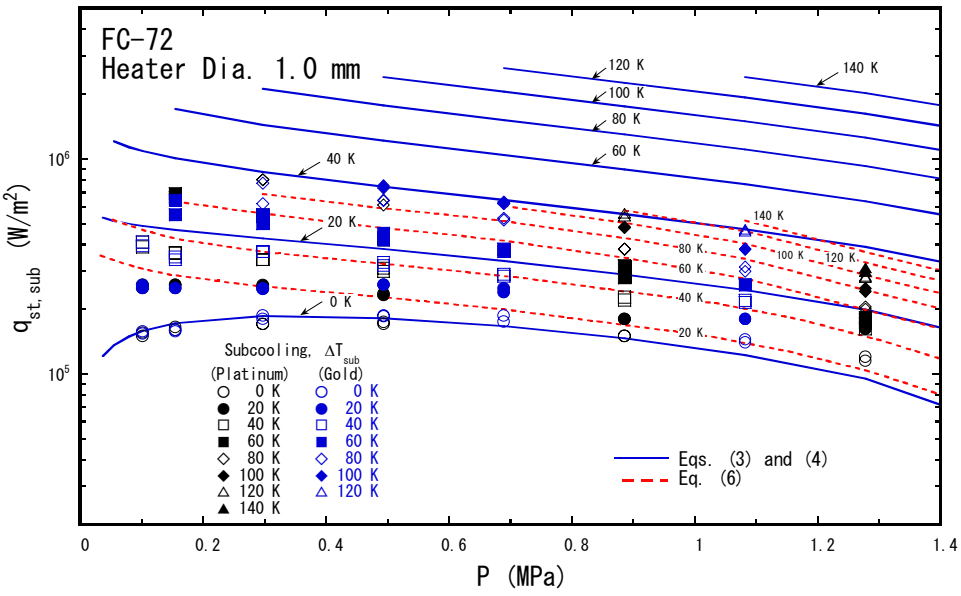

Fig. 5 The Steady-state CHFs for pressures with liquid subcooling as a parameter

4.3.2 Subcooled CHFs for wide ranges of subcoolings and pressures

The steady-state CHFs, $q_{st,sub}$, that were measured on both platinum and gold heaters for a wide range of subcoolings and pressures in a pool of FC-72 due to transient heat inputs are shown in Figs. 4 and 5 for liquid subcooling and pressure parameters, respectively. The $q_{st,sub}$ from both heaters well agree each other for each liquid subcooling at pressures. The CHFs in Figs. 4 and 5 show a significant dependence of pressure and increase with the increase in liquid subcooling.

In Figs. 4 and 5, the corresponding curves of CHFs based on HI are plotted with the blue solid lines. Those corresponding values were obtained from correlations in Eqs. (3) and (4). Equation (3) was given by Sakurai (2000) by modifying the Kutateladze's correlation in Eq. (4) taking into account the non-linear effect of high liquid subcooling. The CHF's correlation based on the HI model expressed by Eq. (3) including Kutateladze's saturated CHF correlation in Eq. (4)[10],[11] did not explain the experimental results at all.

The value of K_1 horizontal cylinder is 0.17, and the K_2 values are derived to express the corresponding values in Eq. (3) for the experimental results. The values of K_2 are dependent on pressure and can be derived from Eq. (5).

$$q_{st,sub} = q_{st,sat}[1 + K_2(\rho_l / \rho_v)^{0.69}(c_{pl}\Delta T_{sub} / h_{lv})^{1.5}] \quad (3)$$

$$q_{st,sat} = K_1 h_{lv}\rho_v(\sigma g(\rho_l - \rho_v)/\rho_v^{\,2})^{1/4} \quad (4)$$

$$K_2 = 0.39(R')^{-0.6} \quad (5)$$

Compared to the corresponding curves by HI model, the experimental data of CHFs, $q_{st,sub}$, appear with a lower of increasing rate at higher subcoolings. They can be seen clearly in Fig. 4 for the $q_{st,sub}$ in each liquid subcooling except at zero subcooling. This phenomenon was suggested due to the lower limit of HSN surface superheat in originally flooded cavities in FDNB regime[5]. The lower limit of HSN surface superheat for a certain subcooling at a pressure is measured as the incipient boiling surface superheat caused by an exponentially increasing heat input during steady-state periods.

An empirical correlation in Eq. (6) was suggested by Fukuda et al. (2004) to express the steady-state CHFs that are due to HSN for liquid subcoolings at pressures above saturated condition, with a constant K_3 depending on pressures. The K_3 values can be calculated from correlation in Eq. (7) that was presented in this study. The corresponding curves obtained from Eq. (6) are shown in Figs. 4 and 5 with the red dash lines.

$$q_{st,sub} = K_3\,\Delta T_{sub}^{\,0.73} \quad (6)$$

$$K_3 = 2.08\times10^4\,(R')^{-1.5} \quad (7)$$

4.4 Transient critical heat fluxes

4.4.1 Transient critical heat fluxes under saturated conditions

Under saturated conditions, the transient CHFs, q_{cr}, for periods, τ, were clearly separated into three groups are the first, second, and third groups. The direct transitions predominantly occur during the short periods of the second group under saturated conditions and were confirmed due to the explosive-like HSN in originally flooded cavities on the cylinder surface.

During short periods, it was observed the independence of q_{cr} generally on pressure for the measurements using the gold heater. On the contrary, the q_{cr} measured on platinum heater were dependent on pressure. More additional discussions in relation to the investigation of transient CHFs under saturated conditions have been reported elsewhere by authors[7].

4.4.2 Effect of pressures on transient CHFs for low and high subcoolings

Figures 6 and 7 show the log-log graph representing values of the transient CHFs, q_{cr}, versus periods, τ, at various pressures under low and high subcoolings of 20 K and 60 K, which were measured on both cylinder heaters. The exponential period, τ, represents the increasing rates of heat input and was ranged from 10 ms up to 20 s.

Both figures show the typical dependence of CHFs on periods. At first, the CHF increases gradually from the steady-state ones, then significantly decreases down to a minimum CHF and finally increases again with the decrease in periods. Those trends remain the typical of three groups of transient CHFs that are separated into the first, second, and third groups, which represent the CHFs measured for long, short, and intermediate periods respectively. The intermediate period is a region of period for the CHFs that lie between the long and short periods in the graph of q_{cr} versus periods, τ.

The CHFs at quasi-steady-state periods of the first group that were obtained from each cylinder heater show an almost similar of increasing rate and well agree each other. At low subcoolings for whole range of pressures from atmospheric to 1278.1 kPa, they can be expressed generally by the corresponding values obtained from Eq. (8) that was given by Sakurai (2000) based on $q_{st,sub}$ of HI model. The corresponding values were plotted on Fig. 6 with blue solid lines. At high subcoolings and low pressure, the quasi-steady-state CHFs well agree with corresponding values from Eq. (8). However, those for a range of higher pressures above 493.6 kPa at high subcoolings, the q_{cr} show agreed results with the corresponding values obtained from Eq. (9) given by Sakurai (2000), based on $q_{st,sub}$ values in Eq. (3). Those corresponding values of quasi-steady-state CHFs for high subcooling of 60 K from Eq. (8) and Eq. (9) were plotted on Fig. 7 with blue solid lines and blue dash dot lines, respectively.

$$q_{cr} = q_{st,sub}(1 + 0.21\tau^{-0.5}) \tag{8}$$

$$q_{cr} = q_{st,sub}(1 + 0.023\tau^{-0.7}) \tag{9}$$

$$q_{cr} = h_c[\Delta T_i(\tau) + \Delta T_{sub}] \tag{10}$$

$$h_c = (k_l \rho_l c_{pl} / \tau)^{0.5} K_1(\mu d/2) / K_0(\mu d/2) \cong (k_l \rho_l c_{pl} / \tau)^{0.5} \tag{11}$$

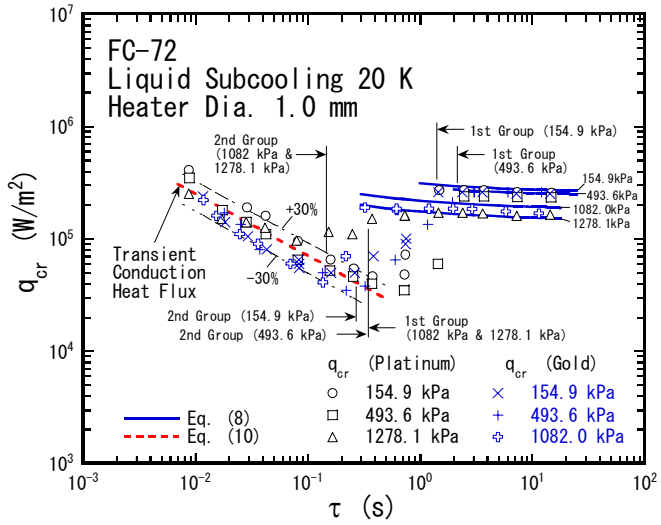

Fig. 6 The relation of q_{cr} and τ for ΔT_{sub} 20 K

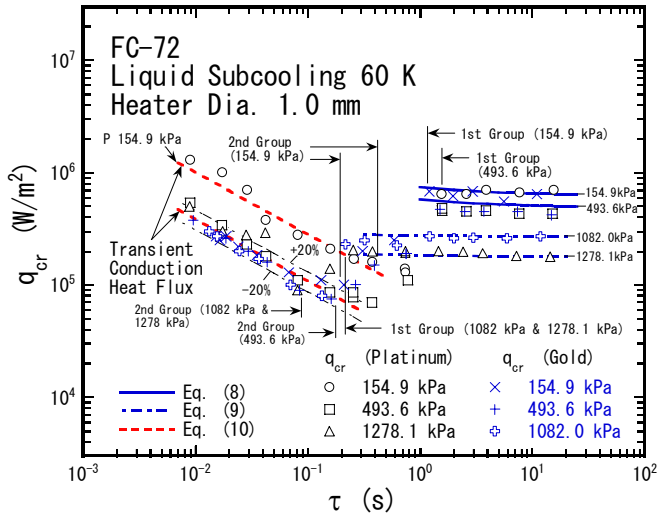

Fig. 7 The relation of q_{cr} and τ for ΔT_{sub} 60 K

The shortest periods belongs to maximum q_{cr} for the first groups shorten with the increase of pressure, except values obtained at pressure of 493.6 kPa. The percentage of increasing value of q_{cr} on both heaters by the increase of liquid subcoolings from 20 K to 60 K at quasi-steadily exponential periods to steady-states ones are in a range of 155%, 80%, 45%, and 20% for pressures of 154.9 kPa, 493.6 kPa, 1082 kPa, and 1278.1 kPa respectively.

During the short periods of the second group, the transient CHFs for period that of due to HSN through the direct transition processes increase with the decrease of periods at pressure. They show an almost similar increasing rate and generally seem to have less dependence on pressures. The prediction values of CHFs within the second group region for various pressures in liquid subcooling 20 K and 60 K were obtained by linear asymptotic lines for period from Eq. (10) and were expressed by red dash lines on Figs. 6 and 7. The asymptote was given by Sakurai and Shiotsu (1977) as a function of the conduction heat transfer coefficient, h_c, for exponential heat input, the incipient boiling surface superheat due to HSN in conduction regime, $\Delta T_i(\tau)$, and the liquid subcooling, ΔT_{sub}. The h_c in Eq. (11) is a function of μ (= $[\rho_l c_{pl}/k_1\tau]^{0.5}$), and K_0 and K_1, which are the modified Bessel functions of the second kind of zero and first orders. The experimental results on liquid subcoolings of 20 K and 60 K during short periods lie within error ranges of ± 30% and 20%, respectively, from the prediction values derived by Eq. (10), which are shown in Figs. 6 and 7. It is considered that the CHFs for short periods of the second group at low or high subcooling conditions can be expressed by Eq. (10).

However, during measurements on platinum heater at pressure of 154.9 kPa and 60 K of liquid subcooling, the transient CHFs belong to short period region of the second group show a higher value compared to other high pressures. It was observed due to the occurrences of the semi-direct transition process induced by the HSN with short nucleate boiling processes then results a slight higher of CHFs.

5. Conclusions

The CHFs in pool boiling of FC-72 due to transient heat input for periods, τ, in a wide range of subcoolings and pressures were measured on a 1.0 mm diameter platinum and gold horizontal cylinders. The results lead to the major conclusions as follows:

1. The typical boiling heat transfer processes remains three types of transition processes are the transition from non-boiling regime to film boiling through FDNB, the direct transition and semi-direct transition, namely type 1, 2, and 3 respectively.
2. The steady-state CHFs obtained from both heaters for wide ranges of subcoolings and pressures well agree each other. At saturated condition, the CHFs almost agree with the corresponding values of CHFs based on the hydrodynamic instability (HI) model. However, in higher subcooling, it was observed that the increasing rate of the steady-state CHFs is lower than the corresponding HI model. This phenomenon was explained by the empirical correlation in Eq. (6) that represents the corresponding CHFs in subcooled conditions due to the lower limit of HSN surface superheat.
3. The transient CHFs for exponential periods, τ, were clearly categorized into three groups are the first, second, and third groups, for long, short, and intermediate periods respectively. Under low and high subcoolings, the quasi-steady-state CHFs of the first group from both heaters well agree each other and give an almost similar of increasing rate at periods.
4. The direct transition and semi-direct transition phenomena observed from the experiment were assumed due to the explosive like heterogeneous spontaneous nucleation (HSN) in originally flooded cavities on cylinder surface.
5. The correlation in Eq. (10) was suggested to predict CHFs for low and high subcoolings

at pressures. The CHFs for low and high subcoolings during the short periods were assumed due to HSN and were almost in the similar increasing rates at periods. Generally, they seem to have less dependence on pressures except for the values obtained from platinum heater at pressure of 154.9 kPa at 60 K of liquid subcooling.

References

(1) Fukuda, K. et al., Pool Boiling Critical Heat Flux of Highly Wetting Liquid (In Japanese), *Journal of the JIME*, Vol. 39 No. 10 (2004), pp. 25-32.

(2) Kasakawa, T. et al., Transient Heat Transfer on a Horizontal Cylinder in FC-72, *Advances in Electronic Packaging*, EEP Vol. 26-2 (1999), pp. 1471-1478.

(3) Park, J., Subcooled Pool Boiling CHFs for Various Liquids due to Steady and Transient Heat Input, *Ph.D Thesis*, Graduate School of Science and Technology, Kobe University (2006).

(4) Sakurai, A., and Shiotsu, M., Transient Pool Boiling Heat Transfer, Part 1: Incipient Boiling Superheat, *ASME Journal of Heat Transfer*, Vol. 99 No. 4 (1977), pp. 547-553.

(5) Sakurai, A., Mechanism of Transitions to Film Boiling at CHFs in Subcooled and Pressurized Liquids Due To Steady and Increasing Heat Inputs, *Nuclear Engineering and Design*, Vol. 197 (2000), pp. 301-356.

(6) Fukuda, K., and Sakurai, A., Effects of Diameters and Surface Conditions of Horizontal Test Cylinders on Subcooled Pool Boiling CHFs with Two Mechanisms Depending on Subcooling and Pressure, *Proceedings of 12th International Heat Transfer Conference* (2002), pp. 611-616.

(7) Sutopo P. Fitri et al., Transient Pool Boiling Critical Heat Flux of FC-72 Under Saturated Conditions, *JSME Journal of Power and Energy Systems*, Vol. 1 No. 2 (2007), pp. 178-189.

(8) Sutopo P. Fitri et al., Critical Heat Fluxes in Pool Boiling of FC-72, *Proceedings of 17th International Symposium on Transport Phenomena (ISTP-17)*, CD-ROM (2006), pp. 1-6.

(9) Sakurai, A. et al., A General Correlation for Pool Film Boiling Heat Transfer From a Horizontal Cylinder to Subcooled Liquid, Part 1: A Theoretical Pool Film Boiling Heat Transfer Model Including Radiation Contributions and Its Analytical Solution, *ASME Journal of Heat Transfer*, Vol. 112 (1990), pp. 430-440.

(10) Kutateladze, SS., Heat Transfer in Condensation and Boiling, AEC-tr-3770, USAEC (1959).

(11) Zuber, N., Hydrodynamic Aspects of Boiling Heat Transfer, AECU-4439, USAEC (1959).